

The Influence of Vibration on the Measurement in High Temperature Molten Salt Electrochemical Cell

Seungmin Ohk, Hyeonjune Noh, Galam Seo and Jaeyeong Park*

Department of Nuclear Engineering, Ulsan National Institute of Science and Technology
okstone@unist.ac.kr

1. Introduction

The molten salt reactor (MSR) is one of the promising next generation reactor types (Gen-IV) that adopts the concept of dissolving nuclear fuel into high temperature fluorine or chloride base salt and using it as fuel and coolant at the same time. Since the MSR is not pressurized compared to the pressurized water reactor (PWR), it is possible to secure economic feasibility by reducing the size of the reactor system. In addition, higher operating temperature (773-973K) due to high thermal properties allow the reactor to achieve high power density [1-2].

Along with these advantages, there are also following tasks. Corrosion is one of the most challenging issues to ensure structural integrity during long operating times. In order to secure stability and commercialize it, the development of a technology capable of monitoring internal physical properties in real time is required. In this regard, electrochemical analysis that measures instantaneous electrical signals can be a good alternative. However, immediate response means sensitivity. In the case of actual scale, it may be affected by undesirable effects such as operating pumps and motors, thus it is necessary to identify the undesirable effect through a lab-scale study.

The preliminary experimental study was conducted for a vibrating cell and vibrating electrode in order to confirm the undesirable effect of convection. Diffusion coefficient and mass transfer rate were measured for LiCl-KCl-CoCl₂ at 773K. The results showed that the prediction of concentration of reactant can be different due to the influence of vibration.

2. Background

2.1. Nernst diffusion layer

Nernst diffusion layer is a hypothetical layer, supposed that gradient of ion concentration between the electrode surface and bulk is constant and equal to the true gradient at the electrode-electrolyte interface. The ions travel from the bulk to the electrode by three principle of mechanism: diffusion, migration and convection expressed in Eq. (1). The subscript r represents a reactant participating in the reaction. D is diffusivity of the chemical species, z is valence of ionic species, ∇c is gradient of concentration, F is Faraday constant, R is gas constant, T is absolute temperature, $\nabla \phi$ is gradient of electric potential, c is concentration at bulk fluid and v is flow velocity. The thickness of the layer

varies within the range from 0.1 to 0.001 mm depending on the intensity of convection caused by agitation of the electrode or electrolyte [3]. For the static flow condition, assuming that a concentration gradient occurs and the movement of ions is dominated by diffusion, the thickness of the Nernst diffusion layer can be approximated by Eq. (2) based on the Fick's 1st law.

$$N_r = -D_r \nabla c_r - \frac{z_r F c_r D_r}{RT} \nabla \phi + c_r v. \quad (1)$$

$$\delta_d = D_r \frac{c_b - c_i}{N_d}. \quad (2)$$

2.2. The influence of convection on the electrode

In an electrolysis, the current is decided by how much reactant transport to the electrode. The more reactant approaches, the higher current measures. For the convective flow condition, the bulk convection alone does not cause a net current due to the electroneutrality. Eq. (3) presents reduction current considering only the effect of diffusion. However, as shown in Eq. (4), convection can cause mixing of the solution, and while it alone cannot cause a current, fluid motion can affect concentration profiles and serve as an effective means to bring reactants to the electrode surface [4]. Thus, the convection can regulate the current as the gradient of concentration is influenced by the convection.

$$i_r = z_r F N_d = z_r F D_r \nabla c_r. \quad (3)$$

$$\frac{\partial c}{\partial t} = \nabla \cdot (D \nabla c) - \vec{v} \nabla c. \quad (4)$$

Even under stationary flow conditions, if there is convection that we do not recognize, such as micro-vibration from device or natural convection due to density difference, the actual value may differ from the predicted value.

2.3. The model of diffusion layer for vibrating condition

The vibrating electrode inducing the turbulence have been studied on the metal dissolution or deposition in that they reduce the concentration polarization and enhance mass transfer. Several models have been proposed in order to understand the improvement of mass transfer. Herein four models are widely adopted [5]. Stretched film model (STFLM) assumes that the area where mass transfer is same as the area where the effective area is swept by vibration. This model is valid at high

frequencies and low amplitudes where the thin film state can be maintained. Quasi-steady state (BL, Boundary layer) is intended to predict the boundary layer phenomenon by substituting the flow velocity in the instantaneous state for the steady state. This model has limitation for the condition of high frequencies where the boundary layer can be distorted. The analogy model (BLTH, Boundary layer thinning) is the model to predict the thickness of diffusion boundary layer from the hydrodynamic boundary layer based on the analogy between mass and momentum. The combined model considers the combined effect of oscillating flow and concentration gradient. This model assumes the concentration boundary layer due to the velocity gradient and diffusion gradient are the similar. Eq (5-7) represent the correlations based on each model. Re_v is vibrating Reynolds number, Sc is Schmidt number of the fluid, λ is the empirical constant, l is the length of active surface and a is the amplitude.

$$Sh_{BL} = \lambda Re_v^{0.5} (l/a)^{0.5} \quad (5)$$

$$Sh_{BLTH} = 0.506 Re_v^{0.5} Sc^{0.3} \quad (6)$$

$$Sh_{Comb} = 0.809 Re_v^{0.5} Sc^{0.3} (l/a)^{0.17} \quad (7)$$

3. Experiments

3.1. Methodology

When the voltage is applied, the concentration decreases as the reactive ions are reduced on the surface of the electrode. The generated concentration gradient become reduced by diffusion due to the concentration difference (Fick's law). Since the diffusion rate and current are proportional to the concentration in the bulk solution, it is possible to calculate the concentration based on the measured peak current from cyclic voltammetry through the Eq. (8). i_{peak} is cathodic peak current, F is Faraday constant, n is number of electrons, D is diffusion coefficient, c_0 is bulk concentration, v is sweep rate, R is gas constant and T is bulk temperature. In other words, based on the formula, if the current value and diffusion coefficient value are known, the concentration value also can be calculated.

$$i_{peak} = -0.6105 \left(\frac{F^3 n^3 D c_0^2 v}{RT} \right)^{0.5} \quad (8)$$

3.2. Test apparatus

Figure 1 shows the schematic diagram of the test apparatus. The electrochemical experiments based on three electrode system using molten salt of LiCl-KCl with 0.1 wt% of $CoCl_2$ (Sigma-Aldrich, 99.99%) were conducted under vibration condition. A VersaSTAT3 potentiostat with VersaStudio software was used to apply

potential and measure current. A diameter of 2 mm and a 6 mm tungsten rod were used as working electrode and counter electrode, respectively (Alpha-Aesar, 99.99%). The Ag wire immersed in LiCl-KCl-1wt% AgCl in a Pyrex glass tube with had very thin tip was used as reference electrode. The quartz cell containing the salt and electrodes was placed in an electric resistance furnace installed under the glovebox. The temperature of the cell in furnace was set as 773K and the atmosphere of glovebox was maintained with Argon gas ($P_{O_2} < 2.1$ ppm, $P_{H_2O} < 0.1$ ppm). The cylindrical vibration motors are attached to the top of cathode and top of test tube in order to impose the vibration. The vibration generated as the off-centered pendulum rotated. The rate of motor output was controlled 30%, 60% and 100% using Arduino-Uno. The high-speed camera (Phantom, miro110) was utilized in order to evaluate an amplitude and frequency of vibrating electrode. The shutter speed of the device was set to 1000 fps (frame per second). Based on the visualization data, the analysis of amplitude and frequency was performed by using image j software.

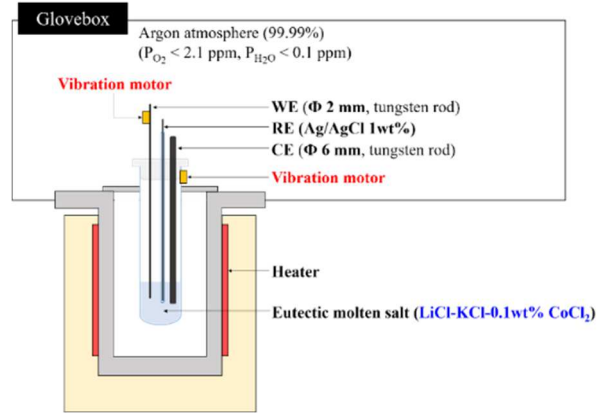


Fig. 1. Schematic diagram of test apparatus.

4. Results and discussion

4.1. Static cell condition

In order to determine the reliability of the cell condition before the vibration experiment, cyclic voltammetry was measured according to the sweep rate for the static cell condition. Fig. 3 shows cyclic voltammogram with varying the sweep rates. The sweep rate is corresponded to 0.025, 0.050, 0.100, 0.200 and 0.300 V/s. It seems reversible condition as the values of peak current had linearity with increasing the sweep rate. Based on the Berzins-Delahay equation (8), the calculated diffusion coefficient is $2.07 \times 10^{-5} \text{ cm}^2/\text{s}$ for the sweep rate of 0.100 V/s. The value is within the range of the results of previous researches.

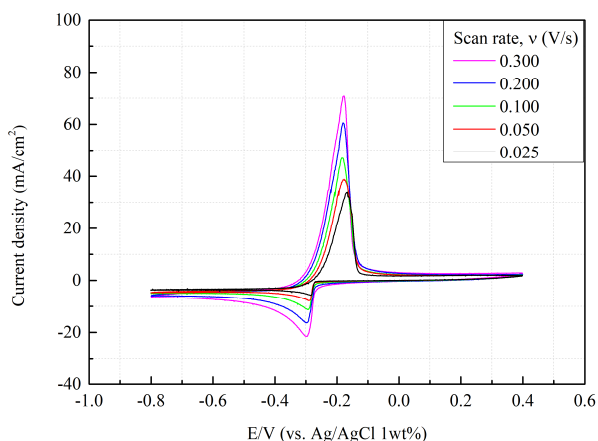


Fig. 2. Cyclic voltammogram of LiCl-KCl-0.1wt% CoCl₂ according to the scan rate for the static cell condition.

4.2. Vibrating cell condition

Figure 3 shows the cyclic voltammogram of vibrating cell conditions. The output of the motor which is installed on the outer wall of the cell was changed to 0, 30, 60, and 100%. The sweep rate is 0.100 V/s. The frequencies are the value that proportionally converted from the number of revolutions of the motor. These are corresponded to 0, 94, 187 and 312 Hz. The measured current density increases as the degree of vibration increases. In the case of the highest vibration condition of 312 Hz, the cathodic peak current increases about 13% compared to the value of static cell condition. This is because the reactant supply to the electrode become more active than in the static cell due to the influence of convection. For 187 Hz and 94 Hz, the increase of current is 5% and 2%, respectively. When the frequency is relatively small, the experimental results shows small different that could be regarded as an experimental error. It seems that the vibration is attenuated as it passes through the bulk due to the indirect applying vibration as the motor installed on the outer wall of the cell.

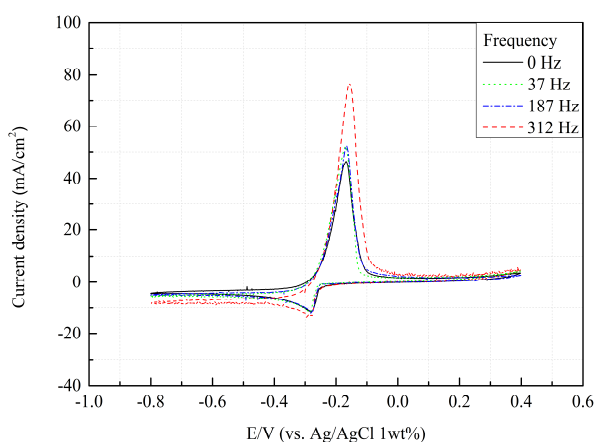


Fig. 3. Cyclic voltammogram of vibrating cell condition according to the frequency for the scan rate of 0.100 V/s.

4.3. Vibrating electrode condition

For the sweep rate of 0.100 V/s, the experiments are conducted with varying the output of motor in the same way as the vibrating cell condition. However, there is a problem that the value measured current exceed the allowable value. It seems that intensified vibrating resulting from the directly imposed vibration on the electrode causes increase in activity of the reaction more enhanced due to the mass transfer more increased. Therefore, the linear sweep voltammetry (LSV) method is adopted and measurement are performed for the low sweep rate.

Figure 4 shows the results of LSV for the vibrating electrode condition. The output of the motor is corresponded to 0, 30, 60 and 100%. For all cases, the sweep rate is 0.010 V/s. The frequencies determined by utilizing high-speed camera are corresponded to 0, 50, 125 and 200 Hz, respectively. As the sweep potential increases, limiting current region is observed. The limiting current density increases as the frequency increases. In the case of 125 Hz, the measured current continuously increases. This is because of the electrode surface due to the reduction resulting from enhanced mass transfer. For the same region, the case for the 200 Hz should not be performed.

The mass transfer rate presents as Sherwood number is calculated with averaged limiting current. The averaging current is used and the range is from -0.3 V to -0.7 V.

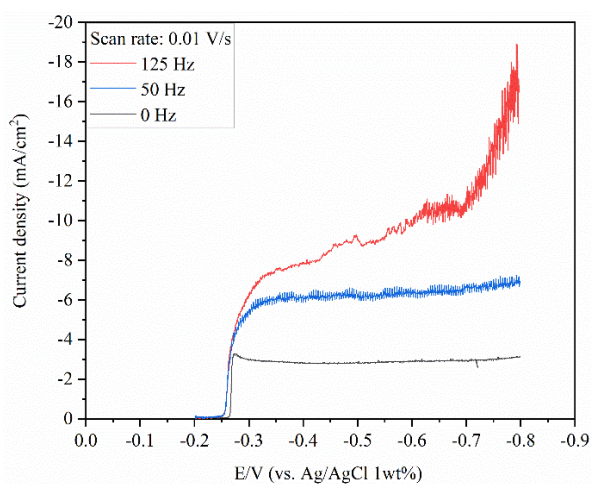


Fig. 4. Linear sweep voltammogram of vibrating electrode condition according to the frequency for the scan rate of 0.010 V/s.

Figure 5 shows comparison of experimental results and theoretical correlations to the result of present study. Each blue, black and red lines represent mass transfer correlations based on the boundary layer model, Eq. (5), (6) and (7), respectively. The dashed line and solid line are the case where the characteristic length is set as surface length and diameter, respectively. Magenta triangle symbol and black square symbol are the

experimental results, conducted for the vertical plate. They are similar to the presented correlations. The blue circle symbol is the results of the present study. The mass transfer rate increases as the frequency increases. This is because the agitated flow due to the vibration has the effect of improving mass transfer. It shows similarity when the characteristic length of the correlation is set to the diameter. It seems that the active surface is in a shape of a cylinder rather than flat plate.

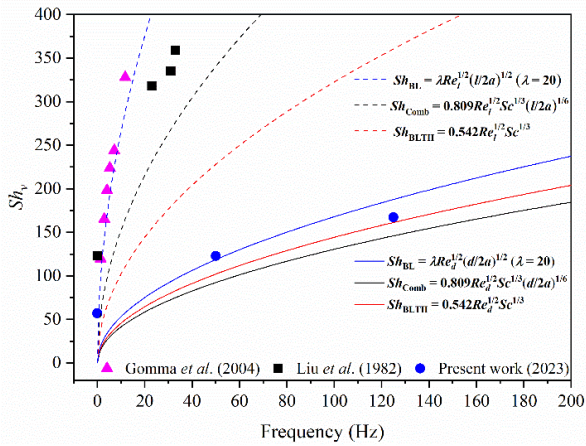


Fig. 5. Comparison of experimental results and theoretical correlations to the results of present study.

5. Conclusion

The influence of vibration on electrolysis investigated experimentally for the molten salt of LiCl-KCl-0.1wt%CoCl₂ at 773K when the vibration was varied. The both diffusion coefficient and mass transfer rate are calculated based on the results of cyclic voltammetry and linear sweep voltammetry. They showed that mass transfer enhanced as vibration intensified. In the case of the vibrating cell, as a result of calculating the predicted concentration based on the diffusion coefficient obtained from the static cell, it was found that the concentration can vary up to 13% as the degree of vibration increased. In the case of the vibrating electrode, it was shown that the mass transfer rate, Sh increased as the frequency increased, which showed a similar trend to the existing correlations.

This research is as a preliminary study, the more work is required to complement the limitation of existing studies and mass transport mechanisms and to better understanding the different transport mechanisms under vibrating conditions.

ACKNOWLEDGEMENT

This work was supported by the Nuclear Safety Research Program through the Korea Foundation of Nuclear Safety (KoFONS), granted financial resources from the Nuclear Safety and Security commission (NSSC), Republic of Korea (No. 220328).

REFERENCES

- [1] Delpech, Sylvie, Molten salts for nuclear applications, Molten Salt Chemistry, Elsevier, pp. 497-520, 2013.
- [2] S. Guo, J. Zhang, W. Wu, W. Zhou, Corrosion in the molten fluoride and chloride salts and materials development of nuclear applications, Progress in Materials Science, Vol. 97, pp. 448-487, 2018.
- [3] J. N. Agar, Diffusion and convective at electrodes, Discussions of the Faraday Society 1, pp. 26-37, 1947.
- [4] J. Newman and K. E. Thomas-Alyea, Electrochemical systems, John Wiley & Sons, 2004.
- [5] H. Gomma, A. M. Taweel, J. Landau, Mass transfer enhancement at vibrating electrodes, Chemical Engineering Journal, Vol. 97, pp. 141-149, 2004.